

BRIEF REPORTS

Brief Reports are short papers which report on completed research or are addenda to papers previously published in the Physical Review. A Brief Report may be no longer than 3½ printed pages and must be accompanied by an abstract.

Monopole strength and shape coexistence in the $A \simeq 100$ mass region

H. Mach,* M. Moszyński,[†] and R. L. Gill
Brookhaven National Laboratory, Upton, New York 11973

G. Molnár[‡]
Institut für Kernphysik, Kernforschungsanlage Jülich, D-5170 Jülich, Federal Republic of Germany

F. K. Wohn, J. A. Winger, and John C. Hill
Ames Laboratory, Iowa State University, Ames, Iowa 50011
 (Received 27 January 1989)

Half-lives of 5.60(15) and 1.58(4) ns were measured for the 0_2^+ levels in ^{100}Zr and ^{100}Mo , respectively, using a β - γ - γ fast timing method. Analysis of the revised $\rho(E0)$ systematics in the crucial $A \simeq 100$ region indicates that high values of $\rho(E0)$ do not by themselves imply strong configuration mixing between two coexisting states as presently assumed.

The abrupt onset of deformation in the $A \simeq 100$ mass region and the accompanying phenomena of coexistence and mixing of spherical and deformed configurations have been extensively studied in the past fifteen years. The strength $\rho^2(E0)$ of electric monopole transitions between 0^+ states has been investigated as a criterion for shape coexistence in neutron-rich Sr and Zr nuclei.¹⁻⁵ This idea was generalized in a recent paper,⁶ in which the anomalously high values of $\rho^2(E0)$ for the $N=60$ isotones ^{98}Sr , ^{100}Zr , and ^{102}Mo were stated to be caused by strong mixing between a deformed ground state and a spherical first-excited 0^+ state.

The present Brief Report reports new lifetimes of excited 0^+ states that clarify conflicting results in the crucial $A \simeq 100$ region. Revised systematics of the $E0$ strength parameter, together with our recent analysis⁷ of the structure of ^{98}Sr and ^{100}Zr , are used here to point out important differences between the various isotones with neutron numbers $N=58-60$ in the shape transitional region and to modify the somewhat oversimplified picture given in Ref. 6.

Measurements were performed at the fission-product separator TRISTAN on line to the BNL High Flux Beam Reactor using a β - γ - γ fast timing technique with electronics optimized for low-energy γ rays.⁸ Fast timing is derived from β - γ coincidences in a thin NE111A plastic scintillator for β rays and a BaF_2 crystal for γ rays, while a desired decay branch is selected from the mass-separated activity using a coincident γ ray observed in a Ge detector. β - γ time resolution (full width at half maximum—FWHM) ranged from 220 ps at 0.2 MeV to 100 ps at 1.3 MeV γ -ray energy. Details of the experi-

mental setup and present data analysis are discussed in Ref. 8. Lifetimes were obtained by the slope method, where the delayed time spectra were χ^2 fitted to an analytical function with a prompt response approximated by a Gaussian.⁸ Due to the well-defined slope, the value of the lifetime is insensitive to the time delay brought by the indirect γ feeding, provided that such a delay is much smaller than the lifetime of interest, as is the case for the lifetimes reported here.

Figure 1 shows the χ^2 fits to the delayed time spectra, and the insets show the key γ - γ cascades. Low-spin β decays of ^{100}Y and ^{100}Nb strongly feed the 0_2^+ states. No significant time delay (< 15 ps) is introduced by a weak indirect γ feeding to the 0_2^+ states, which has been verified⁸ using the centroid shift method. In the case of ^{100}Zr the most significant indirect feeding comes from the 879-keV 2_2^+ state⁵ for which a half-life shorter than 10 ps was determined in the present work. The same limit ($T_{1/2} < 10$ ps) was determined for the half-life of the 1464-keV 2_3^+ level feeding the 0_2^+ state of ^{100}Mo . The latter result is consistent with the more precise value of 2.9(7) ps established⁹ from the recoil distance Doppler method. The lifetimes deduced from the data of Fig. 1 were consistent with those obtained from the time spectra with the gates in the BaF_2 and Ge detectors reversed. [For the latter, no correction was needed for the $T_{1/2}$ of 13 ps (Ref. 10) for the 2_1^+ state on ^{100}Mo , while for ^{100}Zr , we held fixed the independently determined $T_{1/2}$ of 0.55(2) ns (Ref. 7) for the 2_1^+ state in ^{100}Zr .] A weighted average of these 0_2^+ half-life results is included in Table I.

Our results are compared with previous half-lives in

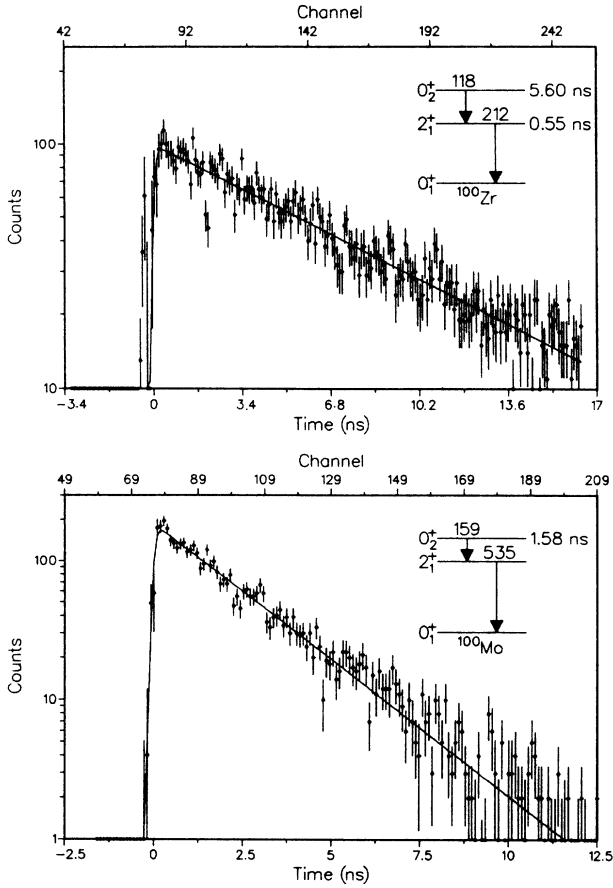


FIG. 1. Top: delayed time spectra for the 0_2^+ level in ^{100}Zr obtained with a 118-keV BaF_2 gate and a 212-keV Ge gate; the χ^2 fit curve is for $T_{1/2} = 5.60$ ns. Bottom: delayed time spectrum for the 0_2^+ level in ^{100}Mo selected with a 159-keV BaF_2 gate and a 535-keV Ge gate; χ^2 fit is for $T_{1/2} = 1.58$ ns.

the third column of Table I. Our new ^{100}Mo 0_2^+ half-life (obtained by the very reliable slope method) resolves a discrepancy between Ref. 14 and the earlier measurements of Refs. 10–12 in favor of the latter. [The techniques used were Coulomb excitation,¹⁰ delayed coincidences¹¹ (with a poor time resolution), and recoil distance Doppler shifts.¹²] Our result strongly disagrees with the 3.0(1) ns of Ref. 14 obtained by a delayed coincidence method but with a time resolution an order of magnitude inferior to that of our measurement. The strong disagreement between Ref. 14 and the other studies implies a systematic error in the experiment of Ref. 14. In the case of ^{100}Zr , our new half-life does not support the earlier measurement of Ref. 2 that was also obtained by a delayed coincidence method but with a much inferior time resolution. [During revision of the present paper we became aware of more recent results: $T_{1/2} = 1.65(4)$ ns (Ref. 15) for ^{100}Mo , obtained by the same method used in our work, and $T_{1/2} = 5.36(23)$ ns (Ref. 16) for ^{100}Zr , obtained by the centroid shift method, both of which are in very good agreement with our results.]

Newly calculated values of the transition strength $\rho^2(E0)$ are included in the fifth column of Table I, together with the branching ratios used in the calculations. [The $\rho^2(E0)$ values were obtained using well-known formulas¹⁷ and tabulated electronic factors.¹⁸] For ^{100}Mo the new $\rho^2(E0)$ value is twice as large as the latest reported value¹⁴ due to the different $T_{1/2}$ values. For ^{100}Zr the new $T_{1/2}$ and branching ratio⁵ values differ from previous data,² resulting in a net 40% reduction of the old $\rho^2(E0)$ value.² Since the new results affect the $\rho^2(E0)$ systematics of Ref. 6, we have replotted $\rho^2(E0, 0_2^+ \rightarrow 0_1^+)$ in Fig. 2 for even-even nuclei in the $A \approx 100$ region. Contrary to Fig. 4 of Ref. 6, the $^{100}\text{Zr}_{60}$ point is no longer the largest one

TABLE I. $T_{1/2}$ and $E0$ results for 0_2^+ states in selected $N = 58-60$ isotones.

	E_{1ev} (keV)	$T_{1/2}$ (ns)	Branching ratio	$\rho^2(E0)$	X_{211}	Ref.
$^{100}\text{Mo}_{58}$	695	1.58(4)		0.032(2) ^a		This work
		1.7(2)	$I(E0)/I(E2) = 0.110(8)$	0.042(6)		11
		1.46(50)	$I_k(E0)/I_k(E2) = 0.759(45)$	0.046(12)		12
		1.8(5)				13
		3.0(1)	$I_k(E0)/I_{tot} = 0.0712(36)$	0.016(1)	0.0116(6)	10
		1.65(4) ^d				14
$^{102}\text{Mo}_{60}$	698	0.028(11)		0.12(5)		12
			$I_k(E0)/I_{tot} = 0.00478(78)$		0.062(1)	14
$^{100}\text{Zr}_{60}$	331	5.60(15)		0.092(20) ^b		This work
		3.37(30)	$I(E0)/I(E2) = 1.05$	0.243(15)		2
			$I(E0)/I(E2) = 0.47(10)$	0.16(3)		5
		5.36(23) ^d				16
$^{98}\text{Sr}_{60}$	215	25(2)	$I_k(E0)/I_k(E2) = 1.14(3)$	0.053(9)		3
					0.031(1) ^c	3,7

^aCalculated with branching ratio from Ref. 14.

^bCalculated with branching ratio from Ref. 5.

^cCalculated with branching ratio from Ref. 3 and 2_1^+ half-life from Ref. 7.

^dReported after the present paper was submitted; included during revision.

and the local minimum at $^{100}\text{Mo}_{58}$ has disappeared. Also, we found the $^{98}\text{Sr}_{60}$ value from Ref. 3 to be smaller than the incorrect value that was inadvertently used in Fig. 4 of Ref. 6.

Considering the $N=60$ isotones, for which the maximum $\rho^2(E0)$ values are attributed⁶ to strong mixing of spherical and deformed configurations, it is clear from Fig. 2 that only the ^{100}Zr value, and perhaps the ^{102}Mo value, are similar to the large $E0$ strengths found in this mass region for $0_3^+ \rightarrow 0_2^+$ transitions. The difference between the ^{98}Sr and ^{100}Zr values is especially striking in view of the similar behavior of their 0_2^+ energies.²⁷ Moreover, according to our recent coexistence analysis,⁷ these two isotones have very similar structures since each has 0_1^+ and 0_2^+ states whose properties indicate weak mixing (11–14%) of a strongly deformed ($\beta \sim 0.4$) 0^+ state and a weakly deformed ($\beta \sim 0.2$) 0^+ state. However, there is no contradiction in this, since even in the simplest model for shape coexistence the $E0$ strength depends not only on the mixing amplitudes but also on the difference between the mean square radii for the two coexisting shapes.^{26,6}

To show this explicitly, let θ be the mixing angle (so that the two mixing amplitudes are given by $a = \sin\theta$ and $b = \cos\theta$) and let the two deformations be β_1 and β_2 . Then, with the $E0$ operator expanded to second order in deformation,

$$\rho^2(E0) = (3Ze/4\pi)^2 a^2 b^2 (\beta_1^2 - \beta_2^2)^2. \quad (1)$$

This expression reduces to Eq. (2.15) of Ref. 6 for maximal mixing (i.e., $a^2 = b^2 = 0.50$, or 50% mixing) and when $\beta_1 \gg \beta_2$.

There are two interesting aspects of the $\rho^2(E0)$ systematics of Fig. 2 to consider. Firstly, it is easy to verify numerically that even the highest $\rho^2(E0)$ values in Fig. 1 are in fact rather moderate since Eq. (1) allows for much higher values of $\rho^2(E0)$ for the case where both strong mixing and large differences in the deformations are simultaneously present. Secondly, the moderate $\rho^2(E0)$ values of ~ 0.1 (in units of e^2) can be explained by nearly any mixing, from very weak to maximal. A $\rho^2(E0)$ of 0.1 (for $Z \approx 40$) can occur for very weak mixing provided that the difference between the two deformations is large enough. To illustrate this, let $\beta_1 = 0.4$ and $\beta_2 = 0.1$, then a mixing of only 5% ($a^2 = 0.05$) is enough to give a $\rho^2(E0)$ of 0.1. Maximal mixing also gives a $\rho^2(E0)$ of 0.1 for a smaller (but still quite significant) difference in the deformations, such as $\beta_1 = 0.30$ and $\beta_2 = 0.15$.

The present data on the $N=60$ isotones and the expression for $\rho^2(E0)$ thus clearly show that, contrary to the conclusions of Ref. 6, the strength of the $E0$ transition alone is not a unique indicator of the amount of configuration mixing. In fact, both $N=60$ isotones ^{98}Sr and ^{100}Zr , even though they have $\rho^2(E0)$ values much higher than the average in the region, are characterized by rather weak configuration mixing of 10% and 14%, respectively.⁷

Concerning the third $N=60$ isotone, ^{102}Mo , the large error in the $\rho^2(E0)$ value (due to the imprecise lifetime) prevents a reliable interpretation. However, the ratios

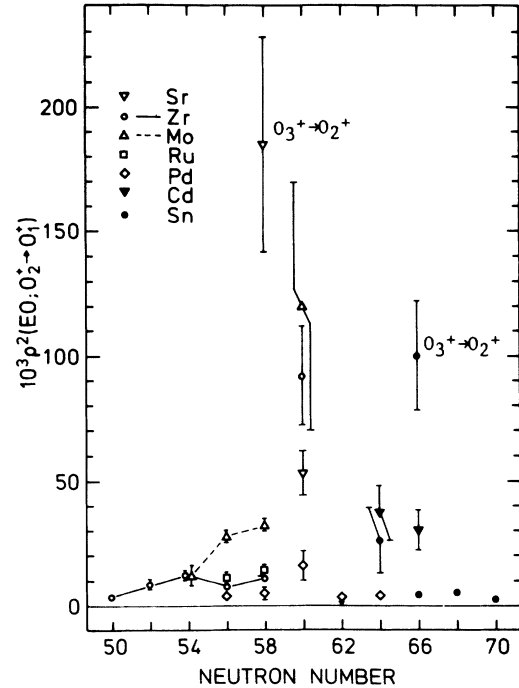


FIG. 2. Systematics of the $\rho^2(E0; 0_2^+ \rightarrow 0_1^+)$ strength for even-even nuclei in the $A \approx 100$ mass region. Data are from Refs. 19 and 20 or as follows: $^{90-96}\text{Zr}$ (Ref. 21); ^{102}Mo (Ref. 14); ^{102}Ru (Ref. 22); $^{102,104}\text{Pd}$ (Ref. 23); $^{108,110}\text{Pd}$ (Ref. 14); $^{112,114}\text{Cd}$ (Ref. 24); and the present work for ^{100}Mo and ^{100}Zr . The $0_3^+ \rightarrow 0_2^+$ values for ^{96}Sr (Ref. 25) and ^{112}Sn (Ref. 26) have also been added.

X_{211} [defined by $X_{211} = B(E0; 0_2^+ \rightarrow 0_1^+) / B(E2; 0_2^+ \rightarrow 2_1^+)$, with $B(E0; 0_2^+ \rightarrow 0_1^+) = e^2 R^4 \rho^2(E0; 0_2^+ \rightarrow 0_1^+)$] given in Table I are more precise than the $\rho^2(E0)$ values. For the data of Table I, the X_{211} ratios seem to correlate well with the monopole strengths $\rho^2(E0)$. The increase of the X_{211} value for ^{102}Mo with respect to that for ^{100}Mo thus suggests that the monopole strength in ^{102}Mo may well be as large as for the other two $N=60$ isotones.

Provided that the ^{102}Mo $E0$ strength is indeed large, there is a reasonable alternative to the interpretation⁶ based on a coexisting "weakly deformed" state, since large X_{211} and $\rho^2(E0)$ values are typical for β vibrational bands in deformed nuclei.²⁰ It is thus possible that the 0_2^+ state of ^{102}Mo is a β bandhead instead of a coexisting weakly deformed state. Therefore the large X_{211} value of ^{102}Mo could be consistent with either of these two viewpoints. However, the β bandhead viewpoint is supported by IBA2 model calculations,²⁸ according to which rather strong configuration mixing takes place in ^{98}Mo and ^{100}Mo , whereas the two lowest 0^+ states of ^{102}Mo both belong to the same deformed configuration. At least, strong mixing between the lowest two 0^+ states of $^{98}\text{Mo}_{56}$ and $^{100}\text{Mo}_{58}$ is consistent with the observed $\rho^2(E0)$ values that are much larger than the corresponding value of $^{96}\text{Zr}_{56}$ (see Fig. 2) for which this mixing is weak.²⁹ As for the ^{102}Mo case, however, more precise and complete data are needed to clarify the issue.

In conclusion, new half-lives for the O_2^+ states of ^{100}Mo and ^{100}Zr yield values for the EO strength parameter $\rho^2(E0; O_2^+ \rightarrow O_1^+)$ that are substantially different from earlier data. Reanalysis of the systematics confirms that high values of $\rho^2(E0)$ do not necessarily mean strong configuration mixing. Instead it must be recognized that knowledge of the difference between the two deformations is required in order to use $\rho^2(E0)$ values as a viable

indicator of the strength of the configuration mixing between the two coexisting shapes.

We wish to thank K. Sistemich and H. Ohm for very useful discussions. The research was performed under Contract Nos. DE-AC02-79ER10493, DE-AC02-76CH00016, and W-7405-ENG-82 with the U.S. Department of Energy.

*Present address: The Studsvik Science Research Laboratory, S-61182, Nyköping, Sweden.

†Permanent address: Institute for Nuclear Studies, PL 05-400, Swierk-Otwock, Poland.

‡Permanent address: Institute of Isotopes, Budapest, H-1525 Hungary.

¹K. Sistemich, G. Sadler, T. A. Khan, H. Lawin, W.-D. Lauppe, H. A. Selic, F. Schussler, J. Blachot, E. Monnard, J. P. Bocquet, and B. Pfeiffer, *Z. Phys. A* **281**, 169 (1977).

²T. A. Khan, W.-D. Lauppe, K. Sistemich, H. Lawin, and H. A. Selic, *Z. Phys. A* **284**, 313 (1978).

³F. Schussler, J. A. Pinston, E. Monnard, A. Moussa, G. Jung, E. Koglin, B. Pfeiffer, R. V. F. Janssens, and J. van Klinken, *Nucl. Phys. A* **339**, 415 (1980).

⁴K. Kawade, G. Battistuzzi, H. Lawin, H. A. Selic, K. Sistemich, F. Schussler, E. Monnard, J. A. Pinston, B. Pfeiffer, and G. Jung, *Z. Phys. A* **304**, 293 (1982).

⁵F. K. Wohn, J. C. Hill, C. B. Howard, K. Sistemich, R. F. Petry, R. L. Gill, H. Mach, and A. Piotrowski, *Phys. Rev. C* **33**, 677 (1986).

⁶K. Heyde and R. A. Meyer, *Phys. Rev. C* **37**, 2170 (1988).

⁷J. C. Hill, F. K. Wohn, R. F. Petry, R. L. Gill, H. Mach, and M. Moszyński, in *Nuclear Structure of the Zirconium Region*, edited by J. Ebert, R. A. Meyer, and K. Sistemich (Springer-Verlag, Berlin, 1988), p. 64; and H. Mach, M. Moszyński, R. L. Gill, F. K. Wohn, J. A. Winger, J. C. Hill, G. Molnár, and K. Sistemich, *Phys. Lett. B* **230**, 21 (1989).

⁸H. Mach, R. L. Gill, and M. Moszyński, *Nucl. Instrum. Methods A* **280**, 49 (1989); M. Moszyński and H. Mach, *Nucl. Instrum. Methods A* **277**, 407 (1989); H. Mach, M. Moszyński, and R. L. Gill (unpublished).

⁹S. J. Mundy, W. Gelletly, J. Lukasiak, W. R. Phillips, and B. J. Varley, *Nucl. Phys. A* **441**, 534 (1985).

¹⁰*Table of Isotopes*, 7th ed., edited by C. M. Lederer and V. S. Shirley (Wiley, New York, 1978).

¹¹H. R. Andrews, J. S. Geiger, R. L. Graham, S. H. Sie, and D. Ward, *Bull. Am. Phys. Soc.* **17**, 514 (1972).

¹²H. Bohn, P. Kienle, D. Proetel, and R. L. Hershberger, *Z. Phys. A* **274**, 327 (1975).

¹³J. Reisberg, H. Genz, J. Lange, A. Richter, and H.-W. Mueller, *Nucl. Phys. A* **280**, 13 (1977).

¹⁴R. J. Estep, R. K. Sheline, D. J. Decman, E. A. Henry, L. G. Mann, R. A. Meyer, W. Stoeffl, L. E. Ussery, and J. Kantele, *Phys. Rev. C* **35**, 1485 (1987).

¹⁵H. Ohm, M. Liang, G. Molnár, and K. Sistemich, in *The Spectroscopy of Heavy Nuclei (Bristol, 1989)*, Proceedings of the Conference on the Spectroscopy of Heavy Nuclei, Institute of Physics, Conf. Proc. No. 105 (Institute of Physics, Bristol, in press).

¹⁶G. Lhersonneau, H. Gabelmann, N. Kaffrell, K.-L. Kratz, B. Pfeiffer, and the ISOLDE Collaboration, *Z. Phys. A* **332**, 243 (1989).

¹⁷J. Kantele, in *Heavy Ions and Nuclear Structure*, edited by B. Sikora and Z. Wilhelmi (Harwood Academic, London, 1984), Vol. 5.

¹⁸D. A. Bell, C. E. Avelado, M. G. Davidson, and J. P. Davidson, *Can. J. Phys.* **48**, 2542 (1970).

¹⁹P. M. Endt, *At. Data Nucl. Data Tables* **26**, 47 (1981).

²⁰J. Lange, K. Kumar, and J. H. Hamilton, *Rev. Mod. Phys.* **54**, 119 (1982).

²¹R. Julin, J. Kantele, M. Luontama, and A. Passoja, *Z. Phys. A* **303**, 147 (1981).

²²A. Giannatiempo, A. Passeri, A. Perego, and P. Sona, *Phys. Rev. C* **33**, 1024 (1986).

²³M. Luontama, R. Julin, J. Kantele, A. Passoja, W. Trzaska, A. Baecklin, N.-G. Jonsson, and L. Westerberg, *Z. Phys. A* **324**, 317 (1986).

²⁴R. Julin, J. Kantele, M. Luontama, A. Passoja, T. Poikolainen, A. Baecklin, and N.-G. Jonsson, *Z. Phys. A* **296**, 315 (1980).

²⁵G. Jung, Ph.D. thesis, University of Giessen, Germany, 1980 (unpublished).

²⁶J. Kantele, R. Julin, M. Luontama, A. Passoja, T. Poikolainen, A. Baecklin, and N. G. Jonsson, *Z. Phys. A* **289**, 157 (1979).

²⁷G. Molnár, S. W. Yates, E. W. Kleppinger, T. Belgya, B. Fazekas, A. Veres, and R. A. Meyer, in *Symmetries and Nuclear Structure*, edited by R. A. Meyer and V. Paar (Harwood, New York, 1987), p. 237.

²⁸M. Sambataro and G. Molnár, *Nucl. Phys. A* **376**, 201 (1982).

²⁹H. Mach, G. Molnár, S. W. Yates, R. L. Gill, A. Aprahamian, and R. A. Meyer, *Phys. Rev. C* **37**, 254 (1988).